Infrared absorption of porous silicon layers and silicon particle-films

Norbert Kniffler Department of Power Systems, University of Applied Science Mannheim, 68163 Mannheim, Germany, E-mail-address: n.kniffler@hs-mannheim.de, Phone: +49-621-2926564, Fax: +49-621-2926260

Herbert Ruebel and Sven Sommer Former Colleagues and Co-Authors

Abstract

Using TaC filaments for a hot-wire chemical vapor deposition (HWCVD) compact material (substrate temperatures 220°C) and porous, non-compact or void-rich layers (120°C) were produced in a silane-hydrogen atmosphere in the pressure range from 1 Pa to 30 Pa. For high pressures the adhesion of the layers was weak. In this case the thus pulverized silicon particles could be removed from the substrate by an ultrasonic process in an isopropanol bath. The suspension of these silicon particles was spread to form a continuous film, namely a "particle-film".

The infrared (IR) spectra of the compact solid, the original porous layers and a series of temper stages of the particle-films are compared and discussed. The role of H and O atoms in the silicon network is investigated. Thus those structural properties, which may be found out by infrared tools, e.g. the bonding configurations of the Si related bonds of the said materials and some possible chemical reactions are explained.

1 Introduction

The following comprehensive study is a contribution to the subtle physics of materials with disordered structures. It investigates the IR phenomena of "classic" compact disordered material, but also those of porous, non-compact silicon layers and silicon particle-films, some special versions of thin non-crystalline solid films. The hot-wire process used by us to deposit silicon films and powders for suspensions is a well established procedure [1, 2, 3, 4]. We preferred TaC filaments [5] instead of the standard wires made of tungsten (W) or tantalum (Ta). Low substrate temperature and high pressure conditions lead to porous, non-compact layers of such a weak adhesion on the supporting material so that they may be easily removed from the substrate surface. The final processing result were solid films consisting of silicon particles. IR absorption in general exhibit features (modes), which may correspond to the vibrational properties of

atomic arrangements in, for example, molecules just as non-crystalline solids. Therefore we got information about bonding configurations of silicon-hydrogen and silicon-oxygen groups in our layers and films by using infrared transmission measurements. The micro structure (that means the specific local atomic environment and bonding) of the porous layers and so the particles may be responsible for a chemical reaction of the solvent on and between the silicon particle-films.

2 Experimental details

2.1 Preparation

The thin silicon films were prepared by thermal decomposition of the gaseous silicon compound silane (SiH_4), in our special case by "Hot-wire Chemical Vapor Deposition" (HWCVD).

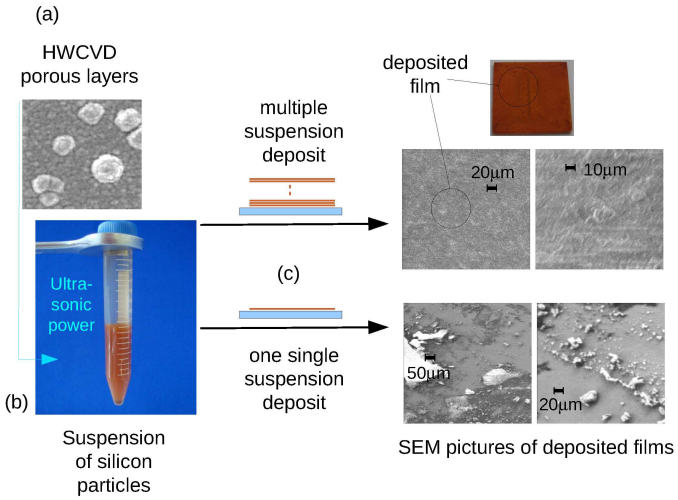

Figure 1: (a) Porous, non-compact layers were grown at a substrate temperature of 120°C and a deposition pressure of 20 Pa on a stainless steel substrate. (b) The substrate was immersed in an ultrasonic bath containing isopropanol to accumulate the silicon material as silicon particles in the bath. (c) This suspension of silicon particles was used to generate a multiple deposit up to a stacked continuous film, demonstrated by several SEM pictures.

Our "hot wires" consist of the metal carbon compound TaC. Advantages of the TaC filament are stability and the attainable high deposition rate. The dimensions of the filament are: diameter 3 mm, length 130 mm. The filament temperature was held constant near 1750°C. The deposition time was adjusted to achieve a relevant thickness of the layers. The base pressure of the UHV

system was $8 \cdot 10^{-6}$ Pa before arranging the SiH_4/ H_2 atmosphere. The hydrogen and the silane flow were kept at 13 sccm. A more compact material (substrate temperature T_S: 220°C) and porous, non-compact layers (T_s: 120°C) in the pressure range of 1 Pa to 30 Pa are produced.

For pressures around 20 Pa and higher the adhesion of the layers was very poor. These porous layers with the aim of the generation of silicon particles were grown at a substrate temperature of 120°C and a deposition pressure of more than 20 Pa on a stainless steel substrate (no special surface treatment) in order to collect a lot of material (see below). After the deposition the substrate was immersed in an ultrasonic bath containing isopropanol for some minutes to accumulate the silicon material as the said silicon particles. The result was a suspension containing particles with a size spread over a range of several micro meters to some nano meters. After 4 weeks a fallout was observed, consisting of the biggest particles, whereas the suspension was still alive. Fig. 1 illustrates the sequence from the weak-adhesive porous layers to a fresh produced suspension which was used to generate a multiple deposit layer by layer up to a stacked continuous film.

2.2 Measurements

Parts of the structural and optical properties are estimated by Scanning Electron Microscopy (SEM) measurements, Optical Transmission Spectra (VIS) and Infrared (IR) Transmission Spectroscopy. In particular: We use a SEM (Zeiss DSM 950) at a moderate operating voltage of 5kV for an introductory structural characterization.

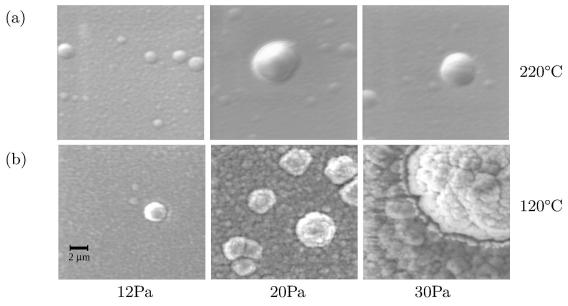

Figure 2: The scanning electron microscopy (SEM) micrographs for representative (a) high (220°C) and (b) low temperature (120°C) samples (The detected "holes" may be due to blistering surface areas).

The optical transmission spectrum was measured by a MAYA 2000 pro in

the range from 200 nm to 1100 nm. Using the procedure of Swanepoel [6] the multiple beam interferences from wavelengths of 700 nm to 1100 nm were used to determine the thickness of the films (The thicknesses of films used for IR measurements are in a range between 5 μm to 10 μm. In the cases without any interference the thickness was roughly estimated via the deposition time).

The IR measurements were done with a Bruker VECTRA 22 in the wavenumber range 400 cm^{-1} to 4000 cm^{-1}.

The IR transmission spectra of the samples processed on untreated silicon wafers were compared with a crystalline silicon reference. A numerical procedure involving the multiple beam interferences of the layer was used to generate a background signal. The multiple beam interference background could be calculated with a linear variation of the optical refractive index over the whole wave number range. To get a more quantitative comparability complementary to the practical approach of comparison of the change of transmission curves we take a look at the absorption coefficient (α) of one relevant and important IR absorption mode of some samples (see below).

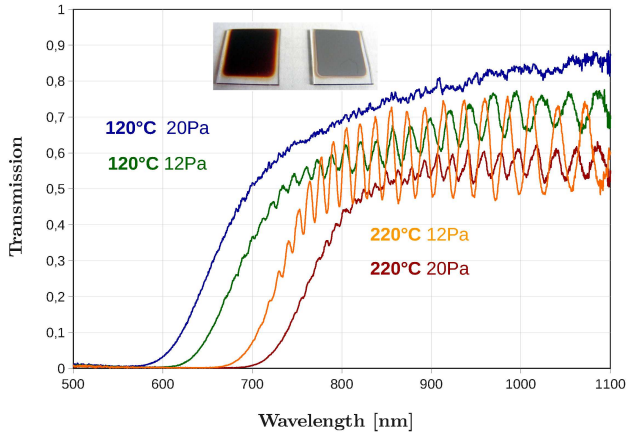

Figure 3: The optical transmission spectra (VIS) for representative low (left inserted picture) and high (right inserted picture) temperature samples.

3 Results and discussion

In a first step we want to describe some indications of the well known discrepancy between dense compact material and porous void-rich layers for our case. Fig. 2 shows SEM photographs in order to compare typical examples of the said compact and porous material. For the compact material inhomogeneities are difficult to detect, because nearly no SEM resolvable microstructure is present (see Fig. 2a), whereas those microstructures are clearly observed in the case

absorption line	low T_S sample [cm^{-1}]	high T_S sample [cm^{-1}]
$O_2 - Si - H_2$ stretching mode [7][11]	2198	2197
$(SiO) - Si - H_2$ stretching mode [7][11]	2152	2150
$Si - H_2$ stretching mode or $Si - H$ at inner surfaces [7]	2085	2077
$O_3 - Si - H$ stretching mode [7][11]	2248	2248
$(SiO_2) - Si - H$ stretching mode [7][11]	2173	2173
$(Si_2O) - Si - H$ stretching mode [7][11]	2118	2114
$Si - H$ stretching mode in a-Si [7,8,10]	2011	1999
ν_{as} $Si - O - Si$ stretching mode in a-Si [10][12]	1050	1049
ν_{as} $Si - O - Si$ stretching mode in SiO_2 [10][12]	990	999
δ_s $(O_2) - Si - H_2$ ip scissors mode (*)	981	980
δ_s $(SiO) - Si - H_2$ ip scissors mode (*)	936	936
δ_s $(Si_2) - Si - H_2$ ip scissors mode [9]	888	880
$\delta_{w,t}$ $(O_2) - Si - H_2$ opp wagging or twisting mode (*)	964	961
$\delta_{w,t}$ $(SiO) - Si - H_2$ opp wagging or twisting mode (*) δ_r $(O_3) - Si - H$ rocking mode [10]	907	903
$\delta_{w,t}$ $(Si_2) - Si - H_2$ opp wagging or twisting mode [9]	841	839
δ_r $(SiO_2) - Si - H$ rocking mode [10]	860	859
δ_r $(SiO) - Si - H$ rocking mode or ν_s $Si - O - Si$ symmetric stretching mode in SiO_2 [10]	795	785
δ_r $(Si_3) - Si - H$ rocking mode [8]	630	630
δ $Si - O - Si$ oop deformation mode in SiO_2 [9] or transverse optical (TO) Si phonon [13]	480	480

Table 1: Peak value wavenumbers of stretching and deformation vibrational modes of Si based bonding configurations which are obvious due to literature or assigned by own fitting (*) used for decomposition of IR spectra of layers deposited at high and low substrate temperature into gaussian shapes of their possible oscillating parts. (abbreviations: ip in plane, oop out of plane; ν stretching mode, ν_s symmetric stretching mode, ν_{as} asymmetric stretching mode, δ_r rocking mode, δ_t twisting mode, δ_w wagging mode, δ_s scissors mode). [Note: The choice of a specific peak value needed for this calculation inherently leads to imprecisions for each used value up to 5 wavenumbers]

of the porous layers (2b)). Additionally we observe, that chemical attack of the latter layers seems easy, an affinity towards oxidation may be expected, see below.

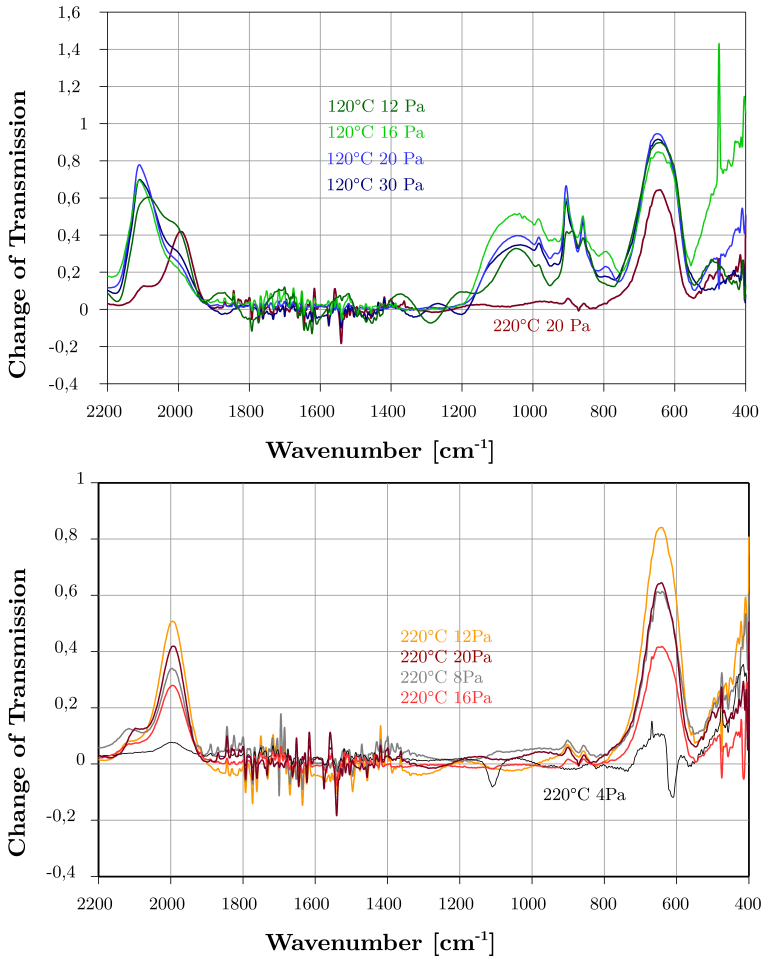

Figure 4: IR transmission of representative layers deposited at substrate temperatures 120°C and 220°C and a deposition pressure range from 12 Pa to 30 Pa.

The VIS spectra in Fig. 3 exhibit intense interference fringes for the examplary high temperature sample (indicating a smooth flat surface) and absence of an interference phenomenon for the low temperature layer (a characteristic of a rough even surface). Therefore we conclude: The transition from a material with a more smooth surface and a suggested homogeneous silicon network (deposition pressure of 1 Pa to 16 Pa and a substrate temperature of 220°C) to porous layers with a rather rough surface and a certainly detectable structural

inhomogeneity (20 Pa, 120°C) is obvious.

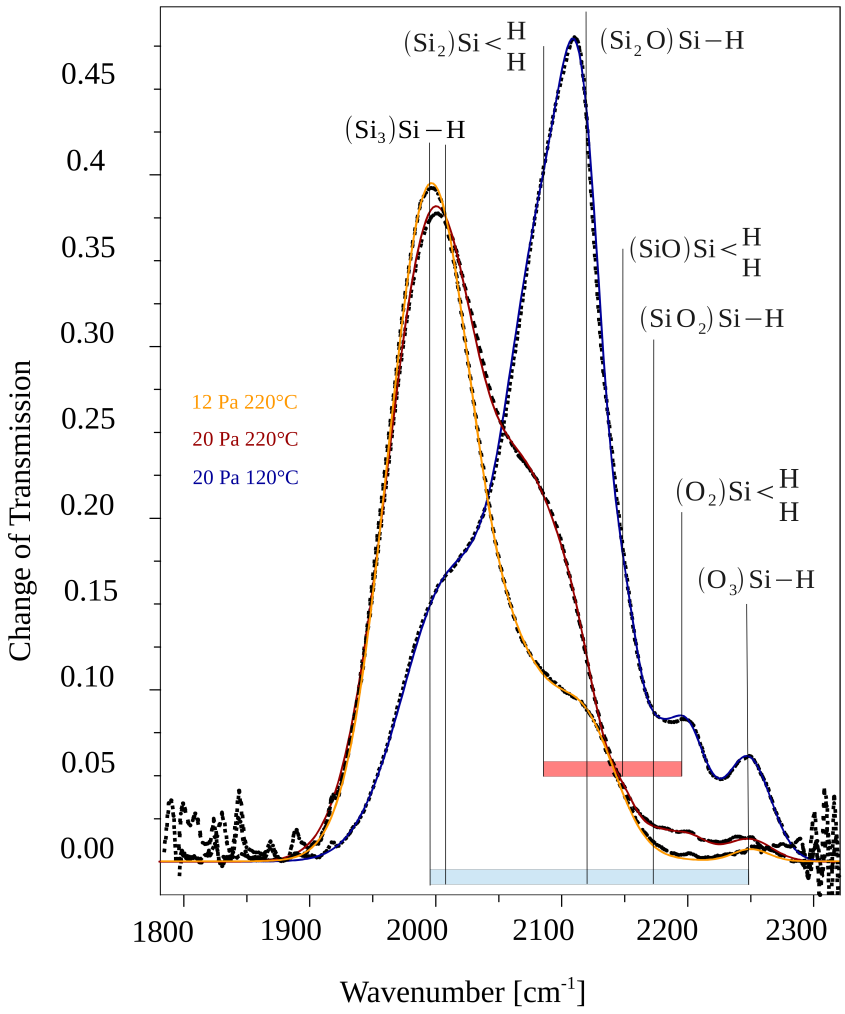

Figure 5: Details of IR transmission of the SiH and SiH_2 stretching regime for low and high temperature samples. The measurement curves (dotted lines) and the sum of the calculated Gaussian decomposition curves (full lines) as denoted (for identification of vibrational modes see Table 1).

For the main part of this work we concentrate our presentation on the essential points of IR data and their discussion.

3.1 Compact and porous silicon material

An overview of the IR transmission spectra is given in Fig. 4: The important differences of these spectra of low and high substrate temperature samples are demonstrated by the quantity of multiple beam interferences, the change from single SiH bonds to SiH_2 units as the main silicon-hydrogen configuration and the relative amount of oxygen content, see below. For simplification of the discussion we define the representative low (120°C) and high (220°C) temperature samples. Table 1 contains the classification of the relevant Si based vibration modes found in the literature [7, 8, 9, 10, 11, 12, 13] coming close to our findings. [Note: The stated positions of absorption maxima slightly differ from publication to publication and therefore generally exhibit a certain spread.]

In the following figures the measurement background is subtracted within the wave number ranges 400 cm^{-1} to 1200 cm^{-1} (Fig. 6) and 1900 cm^{-1} to 2300 cm^{-1}(Fig. 5). A calculation (Gaussian fitting) is made using the peak values of vibrational modes as given in Table 1 to separate the broad measuring curves into the possible parts of vibrational activities. The graphs included in the two figures illustrate the accuracy of the decomposition into the transmission lines corresponding to the denomination in Table 1 compared with the originally determined spectra (measurement: dotted lines; composition of Gaussian functions: full lines): An explicit coherence can be concluded. Please note at this point: A recent more theoretical approach about properties of porous silicon solids ("porous structures")[14] confirms the previous assignments of the main O and H related vibrational modes (Si-O-Si and Si-H vibrations) in non-crystalline silicon based thin films in literature cited and used by us to characterize our porous films. Earlier work on vibrational analysis of silicon-hydrogen species in pure and oxidized porous silicon deposited by electrolysis was done by Ogata et al. [15, 16].

H and O content are estimated qualitatively by the strength and/or the height of the IR absorption modes related to the vibrations of the silicon-hydrogen or silicon-oxygen group, in terms like “more” or “less” and “small” or “large” in order to characterize specific differences of the material species. The high temperature samples contain less hydrogen and the hydrogen is, above all, located in single SiH bonds distributed in the solid (absorption at 2000 cm^{-1}) or located at inner surfaces or voids and in a small amount of isolated SiH_2 groups (small absorption at around 2080 cm^{-1}) indicated by the peak centers of the silicon-hydrogen stretching vibrations [7, 8]. The incorporation of intentionally or unintentionally added oxygen is directly evident by the appearance of a strong and broad absorption feature in the range around 950 to 1050 wave numbers [17](see Fig. 4 and Fig. 6 for this work). The absorption coefficient α determined at the wavenumber value 1050 cm^{-1} may be assumed as a rough but also an appriopriate measure to compare the ratios of the O content of relevant samples, because α also includes explicitly the sample thickness. Table 2 demonstrates the growing O content with decreasing deposition temperature and higher pressure conditions (see also Fig. 4). The O atoms can be embedded in a pure silicon matrix as isolated bond or in a silicon-hydrogen network in-

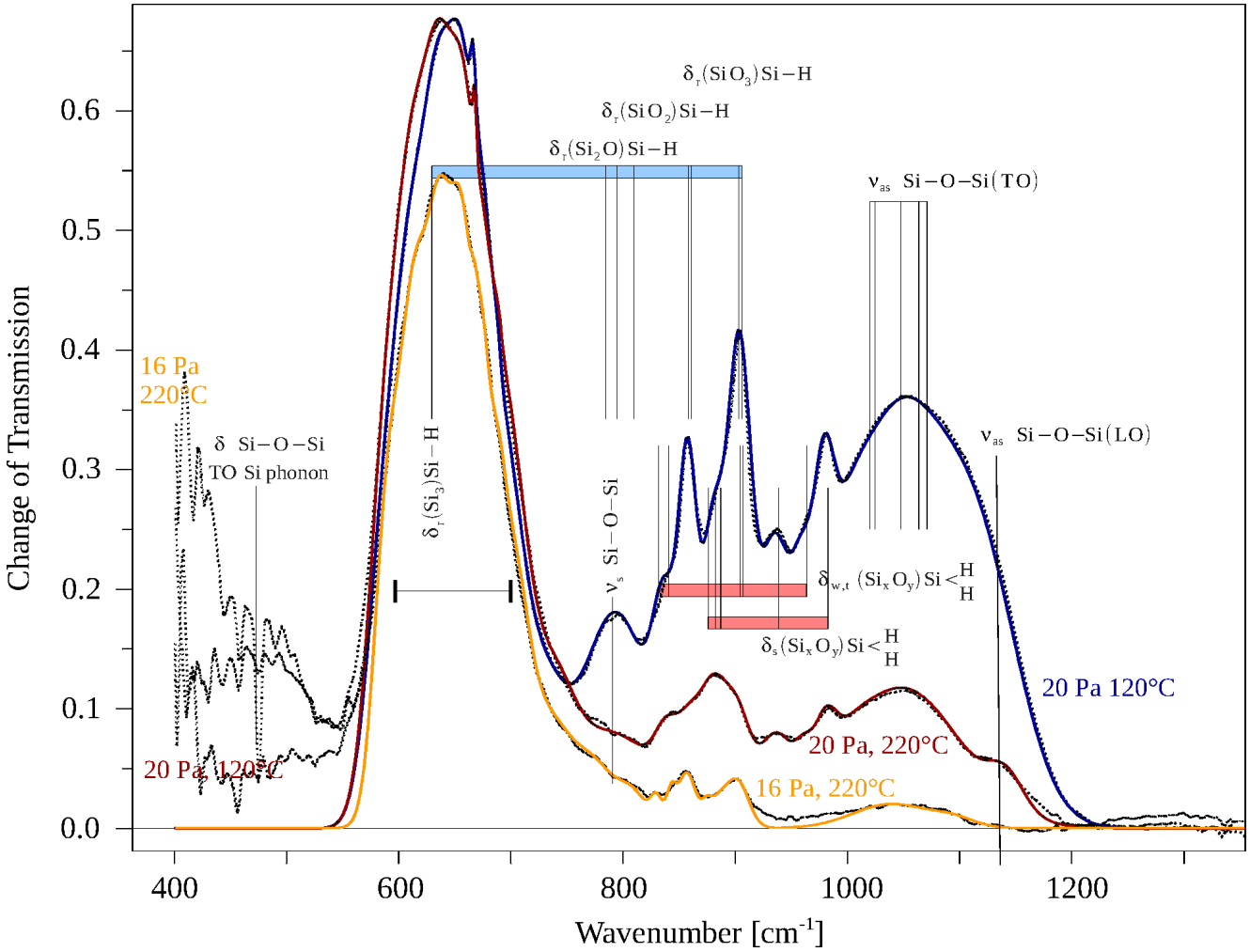

Figure 6: Details of IR transmission of the SiH and SiH_2 deformation regime for low and high temperature samples [(Si_xO_y) denotes the neighboring atom configuration to the SiH / SiH_2 vibrational units]. The measurement curves (dotted lines) and the sum of the calculated Gaussian decomposition curves (full lines) as denoted (peak values for the calculation are quoted from Table 1).

preparation condition	α (1050) [cm^{-1}]
16 Pa, 220°C	33.6
20 Pa, 220°C	112
30 Pa, 120°C	562

Table 2: Absorption coefficient (α) of one relevant and important IR absorption mode: The Si-O bond vibrations indicating 1050 cm^{-1} band of some representative samples.

volving O and H atoms bonded to the same Si atom, with consequences for the values of the vibration energy. The more oxygen atoms are bonded to a SiH or SiH_2 unit (possibly 1-3 for a SiH and 1-2 for SiH_2) the wave numbers of the SiH or SiH_2 stretching vibration absorptions (ν) are shifted to higher values (these findings are observed in figures 4, 5 and 6 and denoted in Table 1).

The high temperature samples possess low content of oxygen as signalized by the lack of (see Fig. 4) or very weak absorption (see Fig. 6) in the said 1050 cm^{-1} wavenumber region and indicated by the absorption coefficient α (see table 2), probably due to a small inner surface area. Depending on the number of O atoms directly bonded to this Si atom small peaks of SiH bond stretching vibrations ν appeared below or near 2100 cm^{-1}in the case of none and above otherwise, ranging from 2100 cm^{-1} to 2250 cm^{-1} ([8, 9, 10], and relevant citations in these publications). In low temperature samples the spectra changed: The features of dihydride arrangements and the presence of surrounding oxygen atoms become stronger leading to a lager amount of oxygen, again signalized by the absorption strength around the 1050 cm^{-1} mode (for discussion of the deformation modes, see below). The relative increasing content of hydrogen as demonstrated by the height of SiH / SiH_2 stretching modes in the stated wavenumber range is in consequence higher for the low temperature samples.

In the following part of our work we want to evaluate the positions of the determined vibrations in terms of local electronegativities of O atoms in the neighborhood of Si atoms. We use the data generated in figures 5 and 6 complying with Table 1. Starting point or better the reference sample or base material is the high temperature sample spectrum, which defines nearly absence of oxygen: the transmission respective the absorption of oxygen related modes is very weak or near the zero line (approximation in figures 7 and 8: The number of oxygen atoms is set to zero N_0=0). All O related modes appear in greater strength for the other inspected samples, especially for the low temperature sample, see above table. Fig. 7 denotes the center wave numbers of the SiH and SiH_2 stretching vibrations in the range of 1900 cm^{-1} to 2300 cm^{-1} as a function of the square root of the number of oxygen atoms N_0 attached to the silicon atom.

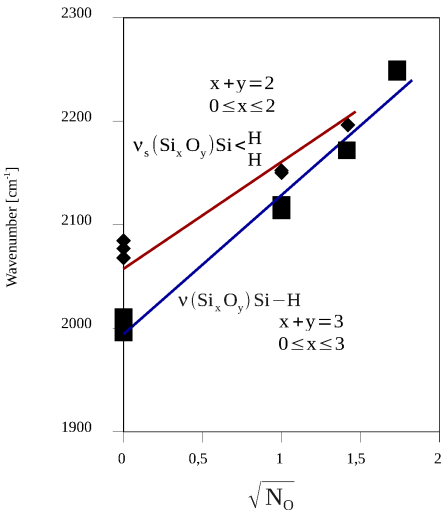

Figure 7: Wavenumber shift of SiH and SiH_2 stretching vibrations depending on the square root of the numbers of oxygen atoms bonded to the SiH / SiH_2 unit [(Si_xO_y) denotes the neighboring atom configuration to the SiH / SiH_2 vibrational units].

Here we assume that the square root of N_0 is proportional to the geometrical mean value of the local electronegativities of the attached oxygen atoms. All stretching modes are fitting to a straight line, which means a linear dependence of $\sqrt{N_0}$. This dependence meets the former assignment of the vibrational modes in Table 1.

While the stretching vibration of the H atom in SiH and SiH_2 units includes a displacement in direction parallel to the Si-H bond (see discussion above), the deformation vibrations on the other side involve in the case of monohydride (SiH) bonding a bending motion (rocking or wagging), in the dihydride (SiH_2) bonding case a scissors bending (δ_s), a rocking (δ_r), a wagging (δ_w) and a twisting (δ_t) motion. A look at these deformation modes of the SiH and SiH_2 vibrations (Fig. 6) reveals: In the 400 cm^{-1} to 1200 cm^{-1} region these vibrations are small for high temperature samples in contrast to low temperature samples, as expected (see remarks above). This behaviour is accompanied by the development of a strong splitting of those absorption modes which indicate more and more SiH_2 sites. In particular: A double peak of wagging, twisting $\delta_{w,t}$ and scissors δ_s deformation vibrations [8, 9] of SiH_2 units is observed and also the rocking (bending) modes δ_r of the SiH units are found. The chemical shift caused by the incorporated oxygen [10, 11, 12, 13, 14] is clearly observed. In

addition we assign the out of plane (oop) deformation vibrations ($\delta_{w,t}$) and in plane (ip) asymmetric deformation vibrations (δ_s) of the (Si,O,H) configuration to practical wavenumber values (see Table 1 and Fig. 6). With these assumptions the dependence of the center line wavenumber value on the number of oxygen atoms leads to a square root function in the case of the δ_r vibration of the SiH bond (Fig. 8(a)) and a linear dependence on the δ_s and $\delta_{w,t}$ vibrations of the SiH_2 bonding configuration (Fig. 8(b)).

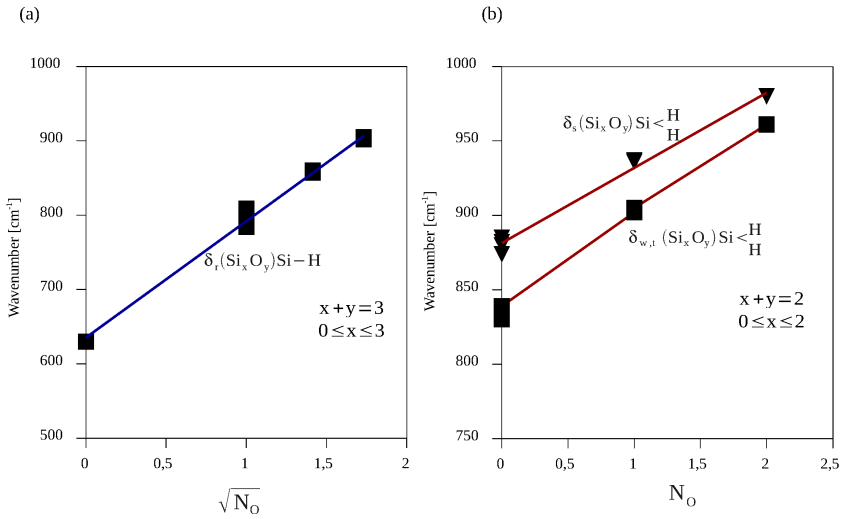

Figure 8: (a) Wavenumber shift of δ_r SiH vibrations depending on the square root of the number of oxygen atoms attached to the SiH bond. (b) Wavenumber shift of δ_s SiH_2 and $\delta_{w,t}$ SiH_2 vibrations depending on the number of oxygen atoms attached to the SiH_2 unit [(Si_xO_y) denotes the neighboring atom configuration to the SiH / SiH_2vibrational units].

The difference can be explained by the assumption of a electrostatic potential between the hydrogen atoms, which is induced by the electronegativity of the neighboring oxygen atoms. Because each polarization is proportional to the square root of the electronegativities and the coulomb potential is proportional to the product of the charges, the wave number shift should be linear.

The findings up to now (Table 1, figures 5 and 6) are compatible with a simple molecular model, which consists of Si-O-Si, SiH and SiH_2 constituents within a ternary (Si,O,H) complex corresponding to the IR active vibrational units of the porous Si-layer. One detail should be added: The intense increase of this certain absorption regime of deformation modes leads to the expecta-

tion, that in a specific complex (see Fig.9) and on account of their spatial and energetic neighborhood the ip Si-O-Si deformation vibration and the oop and ip deformation vibrations of SiH_2 (the 800 to 900 cm^{-1} band and the vibrations from 850 to 950 cm^{-1}) can couple and depending on the two sites bonded to the silicon atoms of this complex, which can be Si or O atoms or both together (see Fig. 9), evoke resonance effects.

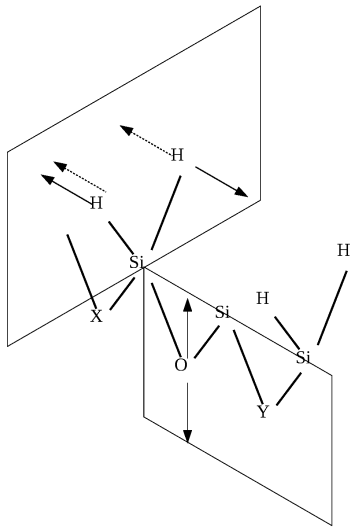

Figure 9: Local microstructure model of a (Si,O,H) complex in porous layers to demonstrate possible deformation vibration mode coupling. Possible displacements of H and O atoms are sketched in (in plane (ip) or out of plane (oop) vibrations). Depending on the sites X and Y (X and Y means Si or O atoms or both together) resonance effects can occur because of overlapping absorption bands/lines.

3.2 Silicon particle - films

The last section comprises the features of silicon particle-films. After their preparation the IR spectra of a series of temper stages of the particle-films were performed. Fig. 10 and Fig. 11 exhibits the detailed spectra of the first (60°C) and the last (220°C) temper stage. All typical lines of SiH, SiH_2 and SiO oscillations similar but somewhat different to porous layers are observed. Obviously vibrational modes of hydrocarbon groups are also found. Figure 10 itself exhibits all characteristic modes of the SiH / SiH_2 stretching mode regime (wavenumber region around 2000 to 2250 cm^{-1}: Fig. 10(a)) and the carbon-

hydrogen CH_z (z=1,2,3) stretching mode regime (wavenumber region around 2800 to 3000 cm^{-1}[18]: Fig. 10(b)).

The SiH / SiH_2 stretching vibration lines are strongly reduced with rising temper temperature mainly due to an effusion of hydrogen. The CH_z stretching modes which orginate from cabon-hydrogen groups of the used solvent (isopropanol C_3H_7OH) taken up by the surface of the Si particle-film nearly disappeared after several temper stages. This disappearance of the CH_z based vibrations and partly the considerable reduction of the SiH / SiH_2 mode ensemble are caused by the "evaporation" of the isopropanol and a reduction of this solvent with parts of the silicon surface-layer by positioning hydrocarbon fragments on the mentioned surface and splitting off some water molecules [19, 20, 21], see Fig. 12.

The decreasing amount of hydrogen bonded to silicon atoms is also observed in the change of the SiH / SiH_2 deformation modes with increasing temper temperature (see Fig. 11). On the other hand this behaviour of the SiH / SiH_2 related modes is accompanied by a more or less increase of the absorption lines near wavenumbers 500, 800 and 1000 cm^{-1} which are attributed to the vibrations within the Si-O-Si triade configuration, see Table 1 and Fig. 11.

Especially the significant strengthening of the 1000 cm^{-1} absorption mode indicates an acceleration of oxidation with increasing temper temperature. Comparing the absorption lines of porous layers and particle-films by a quick view on the intensites of SiH / SiH_2 deformation modes (630 cm^{-1}) and Si-O-Si group (1050 cm^{-1}) related modes clear differences are obvious. Namely the ratio of the SiO mode and the SiH mode is nearly inversed from about 1:2 in the case of porous layers to 1:0,5 for particle-films.

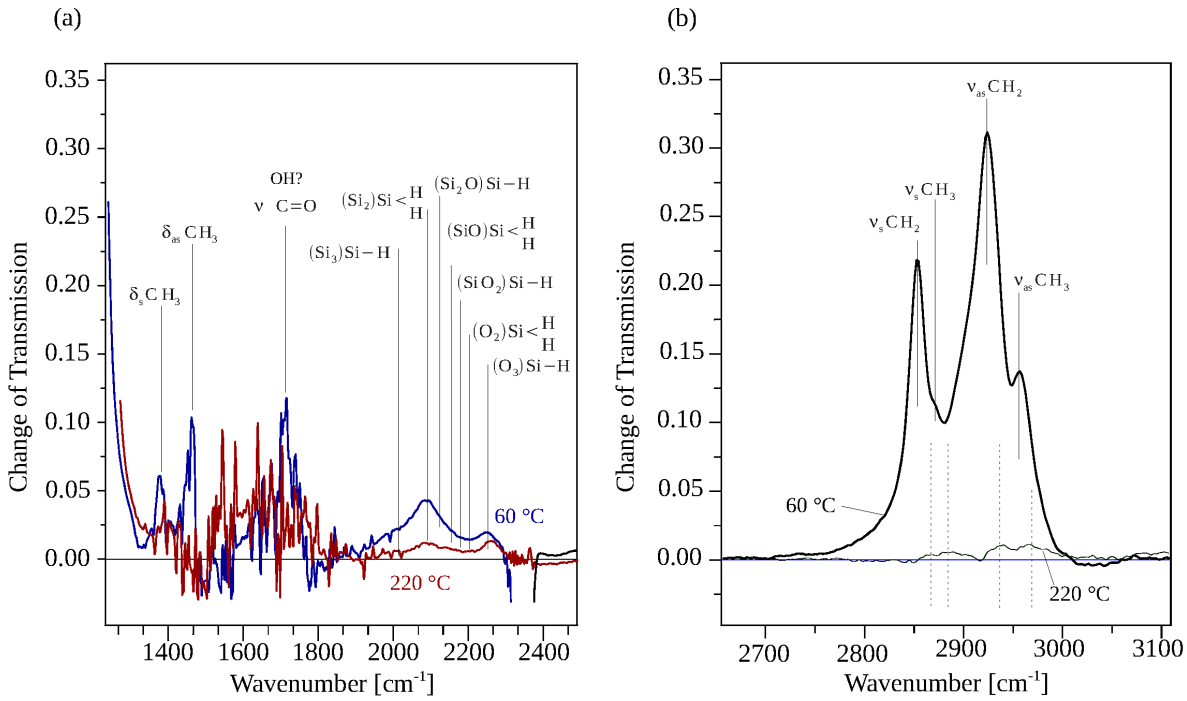

Figure 10: Change of IR transmission of the SiH / SiH_2 (a) and the CH_z (z=1,2,3) (b) stretching mode regimes with growing temper temperatures (60°C and 220°C) for particle-films. The typical CH_z stretching and deformation vibrations are coming from the solvent (isopropanol) [18].

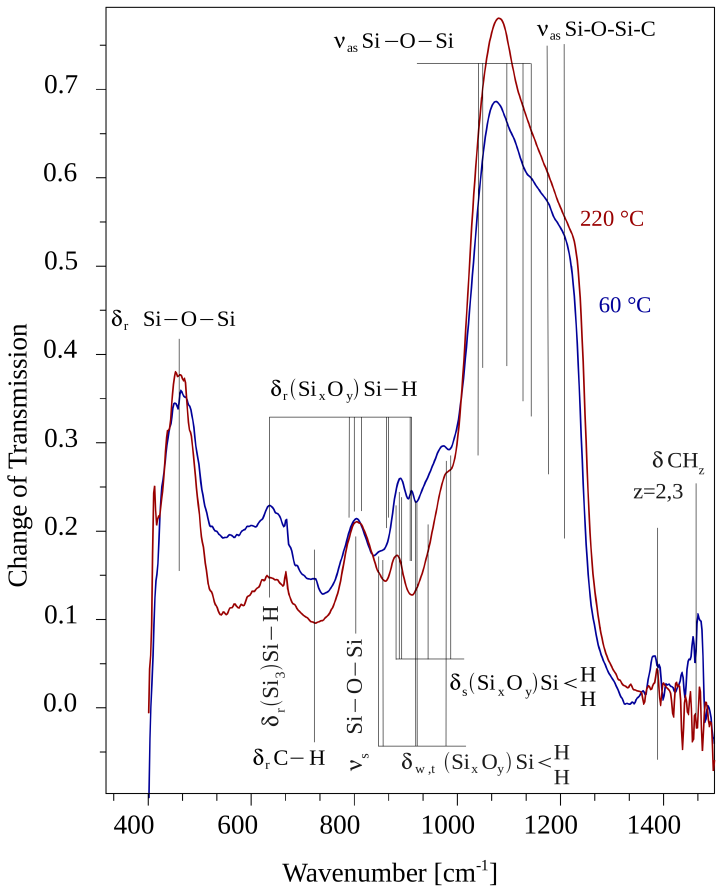

Figure 11: Change of IR transmission of the SiH / SiH_2 deformation mode regime and the Si-O-Si group related modes (see Table 1) with increasing temper temperature (60°C and 220°C) for particle-films.

This means that during tempering of the particle-films a massive amount of oxygen atoms is incorporated in the silicon network instead of hydrogen atoms and therefore a lower hydrogen content compared to porous layers is found.

In addition to the typical oxygen vibrations in a silicon dominated surrounding a vibration feature around 1200 cm^{-1} occurs which can be denoted to a Si-O-Si-C or Si-O-C structure with a hydrogen carbon unit (CH_3), added to the Si-O-Si or Si-O group [19, 20, 21], see also Fig. 12.

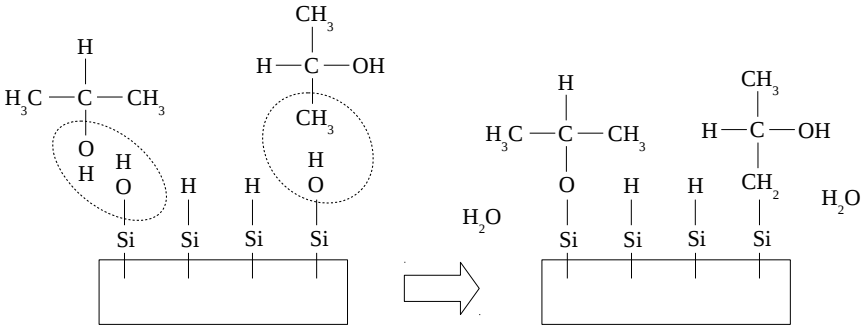

Figure 12: Model of a chemical surface reaction of the solvent (isopropanol) with Si-OH groups of the film particles by splitting off water.

4 Conclusions

The vibrational units and their manifold possibilities of various oscillations which are detectable and identifiable in and by the IR lead to the assumption of a simplified model of the microstructure of the porous Si layers where O and H atoms accumulate in Si-O-Si and SiH/SiH_2 configurations near together. In other words: The essentials of the IR absorption of the porous Si layers exhibit an inhomogeneous material containing univalent H atoms and bivalent O atoms especially within (Si, O, H) complexes. In these cases coupling of certain modes (Si-O-Si and SiH_2 deformation vibrations) and resonance effects may be observed. The matching of the measured IR spectra of stretching and deformation vibrations with the calculated sum of certain single IR absorption lines (Gaussian shapes) given by literature and by own assignment seems to be remarkable.

In the case of a certain number of N_0 oxygen atoms as nearest neighbors of the SiH or SiH_2 vibrational unit (if possible one, two or three O atoms back-bonded) several SiH and SiH_2 vibrational modes are shifted to higher frequencies.

These shifted wavenumber values of the stretching modes of the SiH bonds are proportional to the square root of N_0 as well as those of the rocking (bending) modes of the SiH configuration. By contrast the values of the deformation vibrations of the SiH_2 configurations depend on N_0 directly. The IR vibrations features suggest the noticeable property, that in the case of the particle-films the relative oxygen content is increased in comparison to the original porous layers and an additional distinctive characteristic assignable to a Si-O-Si-C structure appears mostly independent of temper temperature. As a model for the chemical reaction we propose: Si-OH groups or SiH surface "molecules" react with isopropanol splitting off water molecules. In consequence the particles get mechanical contact and additional chemical bridges of Si-O-Si-C bonds are possible.

Acknowledgement

This work was supported by the "Karl Voelker Stiftung" at the University of Applied Science Mannheim. The TaC filaments were donated by Momentive Performance Materials, Strongsville, OH 44149 for testing. The deposition experiments were done within practical exercises of the lecture of the master of science course "Automation Technology and Energy Systems" at the University of Applied Science Mannheim.

References

[1] T. Thovhogi, O. M. Osiele, M. Haerting and D. T. Britton, Phys. Status Solidi C, **1**, 2282 (2004).

[2] M. R. Scriba, C. Arendse, M. Haerting, D. T. Britton, Thin Solid Films, **516**, 844 (2008).

[3] D. T. Britton and M. Haerting, Pure Appl. Chem., **78**, 1723 (2006).

[4] M. R. Scriba, D. T. Britton and M. Haerting, Thin Solid Films, **519**, 4491 (2011).

[5] I. T. Martin, C. W. Teplin, P. Stradins, M. Landry, M. Shub, R. C. Reedy, B. To, J. Portugal, J. T. Mariner, Thin Solid Films, **519**, 4585 (2011).

[6] R. Swanepoel, J. Phys. E: Instrum., **16**, 1214 (1983).

[7] G. Lucovsky, R. J. Memanich, J. C. Knights, Phys. Rev., **19**, 2064 (1979).

[8] M. H. Brodsky, M. Cardona, J. ,J. Cuomo, Phys. Rev. B, **16**, 3556 (1977).

[9] M. Cardona, Phys. Status Solidi B, **118**, 463 (1983).

[10] U. Kahler, Darstellung, Charakterisierung und Oberflaechenmodifizierung von Siliziumnanopartikeln in SiO_2, Ph.D. Thesis (Martin-Luther-University, Halle-Wittenberg, Germany, 2001).

[11] D. Konjhodzic, Optische und elektronische Eigenschaften von Si-Nanopartikeln, Diploma Thesis (University Duisburg-Essen, Duisburg-Essen, Germany, 2003).

[12] S. Musić, N. Filipović-Vinceković, L. Sekovanić, Braz. J. Chem. Eng., **28**, 89 (2011).

[13] H. R. Shanks, W. A. Kamitakahara, J. F. McClelland, C. Carlone, Journal of Non-Crystalline Solids, **59/60**, 197 (1983).

[14] P. Alfaro, A. Palavicini, C. Wang, Thin Solid Films, **571**, 206 (2014).

[15] Y. Ogata, H.Niki, T. Sakka, M. Iwasaki, Journal of Electrochemical Soc., 142, 195 (1995).

[16] Y. Ogata, H.Niki, T. Sakka, M. Iwasaki, Journal of Electrochemical Soc., 142, 1595 (1995).

[17] G. Lucovsky, W. B. Pollard, Journal of Vacuum Science and Technology A1, 313 (1983).

[18] A. Lazauskas, V. Grigaliunas, A. Guobiew, J. Puiso, I. Prosycevas, J. Boltrusaitis, Thin Solid Films, **538**, (2013), 25-31

[19] A. M. Wrobel, A. Walkiewics-Pietrzykowska, P. Uznanski, Thin Solid Films, **564**, (2014), 222-231

[20] R. F. Balderas-Valadez, V. Agarwal, Nanoscale Research Letters, **9**, 508 (2014)

[21] R. Tian, O. Seitz, M. Li, W. Hu, Y. ,J. Chabal, J. Gao, Langmuir, **26**, 4563 (2010).